Int. J. Electrochem. Sci., 11 **(2016)** 8245 – 8255, doi: 10.20964/2016.10.62

International Journal of ELECTROCHEMICAL SCIENCE
www.electrochemsci.org

Green Synthesis of Platinum Nanoparticles Using *Quercus Glauca* Extract and Its Electrochemical Oxidation of Hydrazine in Water Samples

R.Karthik[1], *R.Sasikumar*[1], *Shen-Ming Chen*[1,*], *M. Govindasamy*[1], *J.Vinoth Kumar*[2], *V. Muthuraj*[2],

[1]Electroanalysis and Bioelectrochemistry Lab, Department of Chemical Engineering and Biotechnology, National Taipei University of Technology, No.1, Section 3, Chung-Hsiao East Road, Taipei 106, Taiwan (R.O.C).
[2] Department of Chemistry, VHNSN College, Virudhunagar -626001, Tamilnadu, India**.**
[*]E-mail: smchen78@ms15.hinet.net,

Received: 25 July 2016 / *Accepted:* 28 August 2016 / *Published:* 6 September 2016

Facile, rapid and eco-friendly synthesis of platinum nanoparticles (Pt NPs) using aqueous leaves extract of *Quercus glauca (*Qg) has been reported for first time to detection of environmental and human toxic hydrazine. The as-synthesized Pt NPs were characterized by spectroscopic and analytical techniques. The prepared Pt NPs were around spherical in shape and the size range from 5-15 nm. The electrocatalytic performance of hydrazine has been studied by CVs and amperometric techniques. Interestingly, the Pt NPs modified GCE shows a sharp peak at a very lower onset oxidation potential -0.3 V. The fabricated hydrazine sensor showed very lower detection limit, wide linear range, good sensitivity and excellent selectivity of 7 nm, 0.01 to 283 µM, and 1.704 µA/µM/cm^2 respectively. The green synthesized Pt NPs modified GCE sensor was successfully used for the detection of hydrazine (Spiked) in various water samples.

Keywords: *Quercus glauca,* Eco-friendly, Platinum nanoparticles, Hydrazine

1. INTRODUCTION

Hydrazine (N_2H_2) is one of the main reducing agent for used in industries and agricultures. Hydrazine or its derivatives also widely used in different important applications. Specifically, blowing agents, precursor to pesticides and pharmaceuticals, rocket fuel, corrosion inhibitors, plant growth regulators, fuel cells, gun propellant, catalyst, insecticides and antioxidant etc.,[1]. Hydrazine also considered is highly toxic and very dangerous even in low ppm range to human and environmental in the anhydrous form. So, the U.S. environmental protection agency (EPA) declared and listed hydrazine

is a most priority toxic pollutant. The high level of hydrazine causes diseases in human such as coma, pulmonary edema, seizures, dizziness, nausea and eye, nose, throat irradiation and also severe exposure to damage the central nervous system, kidneys and liver. Not only human, the animal also affected for inhalation of hydrazine may produce liver tumors, dermatitis, spleen and thyroid problems. Finally, severe exposure of hydrazine for continuous 6 months causes death. So, the detection of hydrazine is very necessary. A number of methods have been previously reported to detection of hydrazine including chemiluminescence [2], high performance liquid chromatography (HPLC) [3], spectrophotometry [4], gas chromatography-mass spectrometry and fluorescence [1]. Among them, the electrochemical methods offer a portable, cheap, time consuming, fast, sensitive and selective method for the detection of hydrazine.

Recently, nanomaterials have much attention due to their variety of applications such as energy storage devices, electronic and optical displays, manufacturing of advanced materials, super computers, catalysis, chemical and biosensors, etc., [5-7]. Particularly, noble metal nanoparticles viz Ag, Au, Pd and Pt have wide recognition owing to their potential role in physics, chemistry, material science, biological and medicinal areas [8]. Among them, platinum has high surface area, high melting point (1769 ˚C) and good resistance to corrosion and chemical attacks. It is an efficient catalyst for the reduction of automobile pollution, hydrogen storage material, proton membrane exchange fuel cells, direct methanol fuel cells and so forth. Up to now, various approaches were developed for the synthesis of Pt NPs by different methods such as sol-gel route, chemical precipitation, pyrolysis, hydrothermal synthesis, sol process, vapor deposition and electro-deposition. The aforementioned techniques have some limitations such as multi-step process, high energy requirement and the use of unsafe chemicals. To overcome these problems, plant-mediated synthesis technique is simple, low cost, eco-friendly and commodious route for the synthesis of Pt NPs. Recently, very few reports available for the synthesis of Pt NPs using several plant extracts including *Cacumen platycladi*, *Prunus yedoensis*, *Azadirachta indica*, *Cochlospermum gossypium*, honey, *Diopyroski kaki* [9-14].

In this work, we report herein the facile synthesis of Pt NPs by using *quercus glauca* (Qg) leaves extract for the electrochemical detection of hydrazine for first time. The prepared nanoparticles were confirmed by UV-visible spectroscopy, Fourier-transform infrared spectroscopy (FTIR), X-ray diffraction (XRD) and transmission electron microscopy (TEM). The proposed technique is fast, eco-friendly, cheap, renewable and reproducible. The fabricated Pt NPs modified glassy carbon electrode (GCE) displayed good electrocatalytic activity towards environment and human toxicity hydrazine with good selectivity even in the presence of common metal ions and biologically co-interfering substances.

2. MATERIALS AND METHODS

2.1. Plant materials and chemicals

The fresh leaves of *Quercus glauca* (Qg*)* were collected from National Taipei University of Technology (NTUT), Taipei, Taiwan (Republic of China). Chloroplatinic acid hexahydrate

($H_2PtCl_6.6H_2O$) and hydrazine were received from Sigma-Aldrich Company. All other chemicals were purchased from the same company and used without further purification.

2.2. Preparation of quercus glauca leaves extract

5 g of collected *quercus glauca* leaves were washed with de-ionized water to remove possible impurities and dried for an hour at room temperature. The healthy leaves were finely sliced tiny pieces and boiled with 100 ml DI water for 15 min and cooled at room temperature. Finally, the pure greenish yellow color extract was collected by filtration and stored at 4 ˚C for further use.

2.3. Biosynthesis of Platinum nanoparticles and fabrication on the GCE

In a typical synthesis, 40 ml of pure *quercus glauca* leaves extract was added to the 100 ml of 2 mM $H_2PtCl_6.6H_2O$ solution and stirred for 30 min at 80 ˚C. During the reaction, very dark brownish color was formed which suggests that bio-reduction process is over and the formation of Pt NPs within 30 min. The synthesized Pt NPs were separated out by centrifugation, air-dried and used for further characterization. Before modification, the GCE was polished with 0.05 µM alumina slurry after that, the prepared Pt NPs was dispersed (2 mg/mL) and about 8 µL was drop casted on the GCE surface. Then, it was allowed to dried at room temperature. Finally, the dried GCE was gently washed with DD water to remove the loosely attached molecules. The obtained GCE was used for the further electrochemical measurements. The synthesis route for Pt NPs material and its application as electrochemical oxidation of hydrazine as shown in scheme 1.

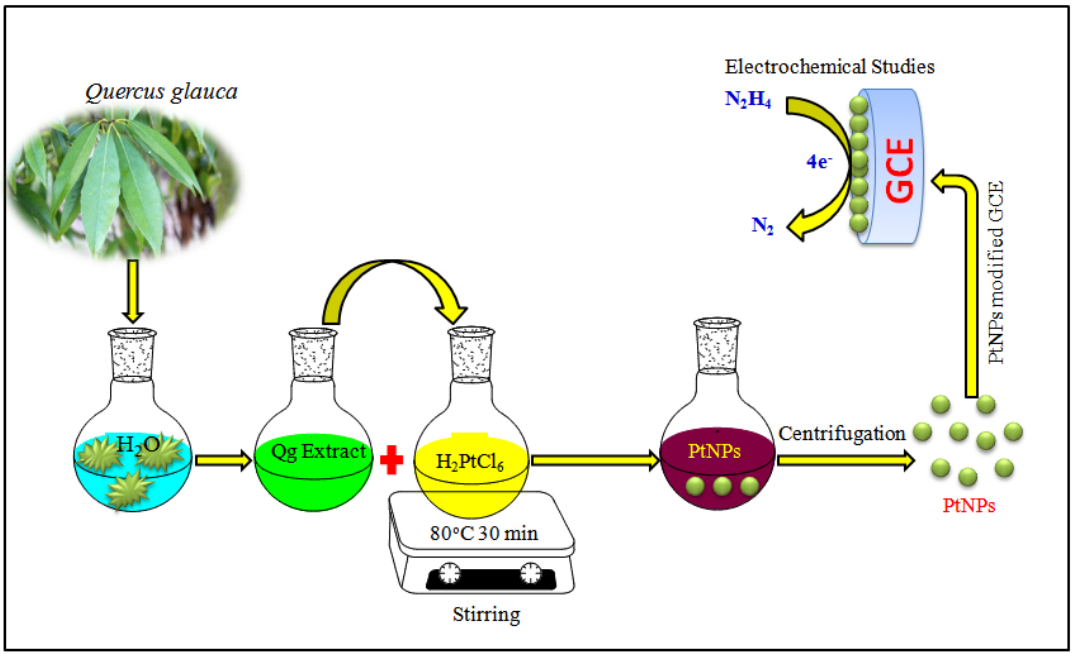

Scheme 1. Synthesis route for Pt NPs material and its application as electrochemical oxidation of hydrazine.

2.3. Characterization

The Pt NPs were characterized by UV-visible spectroscopy (Jasco V-770 spectrophotometer) in the wavelength range of 200-800 nm. The FTIR spectrums of leaves extract and after formation of Pt NPs were scanned (Jasco- FT/IR-6600 spectrophotometer) in the range of 400 to 4000 cm^{-1}. The powder XRD were carried out on a XPERT-PRO (PANalytical B.V., The Netherlands) diffractometer (Cu Ka radiation, k 1/4 1.54 Å). The size and morphology were confirmed by TEM (TECNAI G_2 (Tokyo, Japan). Electrochemical impedance spectroscopy (EIS) studies were recorded using IM6ex ZAHNER (Kronach, Germany). The electrochemical measurements were carried out in CHI 405a electrochemical workstation (CH Instruments Inc., U.S.A) and amperometric (*i-t*) method was measured by AFMSRX (PINE instruments, USA) with a rotating disk carbon electrode (RDCE) having working area of 0.21 cm^2. All the electrochemical studies were measured in a conventional three-electrode system (counter electrode-Pt, reference electrode-Ag/AgCl and working electrode-GCE (area 0.071 cm^2)). All the electrochemical measurements have been executed at room temperature.

3. RESULTS AND DISCUSSION

3.1. Characterization of the PtNPs

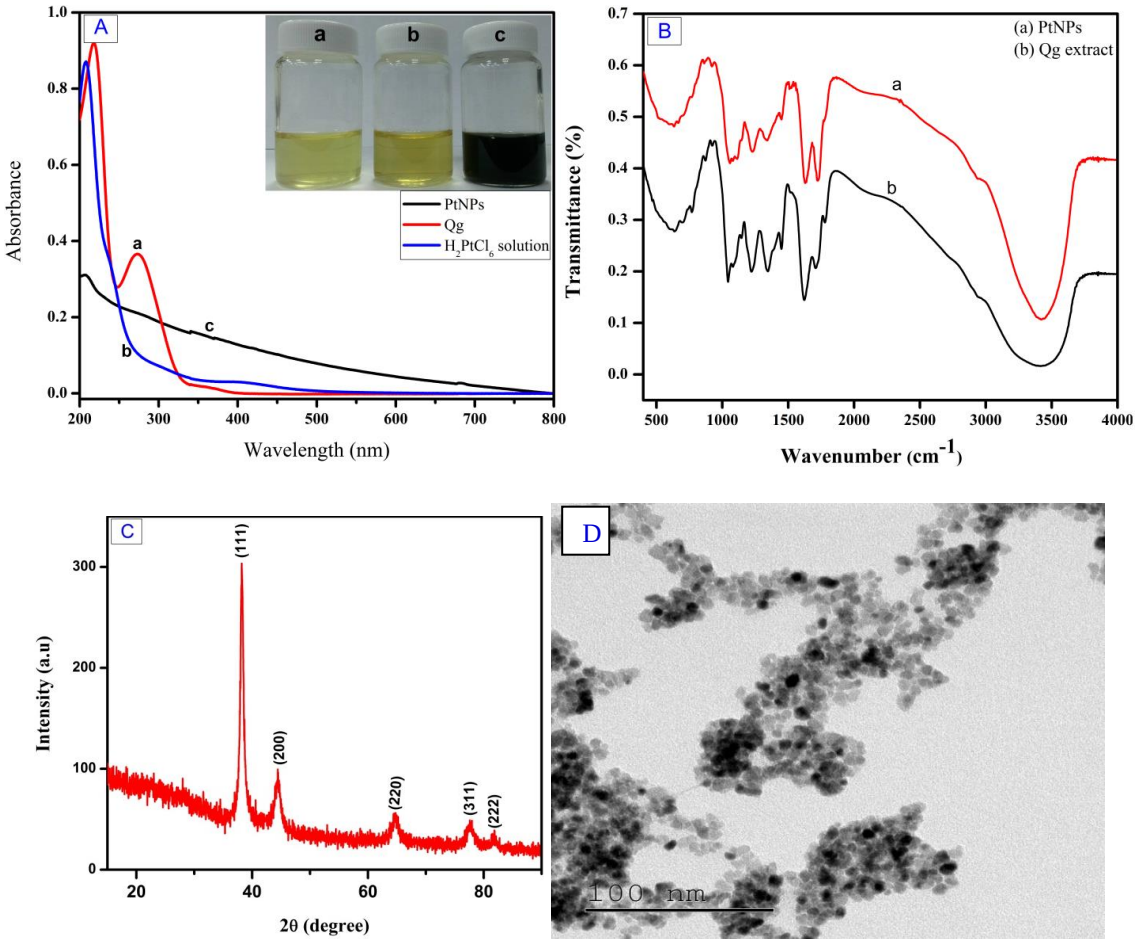

Figure 1. (A) UV-visible spectrum of Qg (a) H_2PtCl_6 solution (b) and Pt NPs (c). (B) FTIR spectrum of Qg pure (a) Pt NPs (b). (C) XRD pattern of Pt NPs. (D) TEM image of Pt NPs.

UV-vis spectroscopy is one of the most simple and commodious technique to identify the formation of Pt NPs and shown in Fig.1A. The $H_2PtCl_6.6H_2O$ shows the absorption peak at around 210 nm (Fig1A(a)) is due to the ligand-to-metal charger-transfer transition between Pt^{4+} and Cl^- ions and the plant extract exhibits the peaks at 217 and 273 nm (Fig1A(b)). After the addition of Qg extract into the $H_2PtCl_6.6H_2O$, the color of the solution was changed from light yellow to dark brown (inset: Fig1A). There was no other discernible peak observed in the UV-vis spectra (Fig1A(c)) and the absorption value increased with the decrease of wavelength, which clearly confirmed the complete reduction of Pt (IV) ions to Pt NPs.

FTIR spectroscopy was carried out to find out the possible biomolecules in Qg responsible for the synthesis and stabilization of Pt NPs and shown in Fig.1B. FTIR spectra of Qg (Fig.1B (a)) showed the bands at 3410, 1732, 1626, 1347, 1226 and 1042 cm^{-1}. The broad band at around 3150-3550 cm^{-1} attributed to the -OH groups of phenolic compounds (flavonoids), tannins and –NH stretching of proteins. The peaks at 1732 and 1626 cm^{-1} represent the C=O stretching of carboxylic acids and primary amines respectively. The bands at 1347 cm^{-1} correspond to the C-H bending vibrations of CH_2 where as bands at 1226 and 1042 cm^{-1} respectively relevant to C-N stretching of aliphatic amine and C-O-C stretching of ether or glycoside groups [15, 16]. After reduction with Pt ions, the intensity and strength of all the peaks are evidently undermined and the shifts of some peaks observed in Fig.1B (b). From the above results, the functional groups such as flavonoids, tannins, carboxyl, amino and glycosides or ether groups are mainly responsible for reduction and stabilization of Pt ions to Pt NPs.

The crystalline structure and phase purity of as-synthesized Pt NPs were determined by X-ray diffraction analysis (XRD). Fig.1C depicts the XRD pattern of Pt NPs synthesized by using Qg extract. The five distinct diffraction peaks in the 2 theta range at 38.4, 44.7, 65.1, 77.9 and 82.2 corresponding to the (111), (200), (220), (311) and (222) respectively. The crystallographic plane of platinum is face-centered cubic (fcc) (JCPDS #87-0644). There is no other noticeable peak were detected, demonstrating that as-synthesized Pt NPs had high crystalline nature. The TEM provides detail about shape, size and morphology of green synthesized Pt NPs which is shown in Fig.1D the image clearly indicates that Pt NPs have nearly spherical in shape and the particles size around 5-15nm.

3.2. Electrochemical impedance spectroscopy studies

Electrochemical impedance spectroscopy (EIS) is one of the most important techniques for identifying the interfacial property of chemically modified electrodes [17]. Fig.2A reveals the nyquist curve of bare GCE (a) and Pt NPs/GCE (b) containing 0.1 M KCl solution with 5 mM $[Fe(CN)_6]^{3-/4-}$. From the curve bare GCE (a) shows a very low semicircle it's due to the less electron transfer resistance compared than Pt NPs/GCE. The Pt NPs/GCE has much larger semicircle its due to the higher electron transfer resistance (b), which clearly indicates the green synthesized Pt NPs was successfully immobilized on the GCE surface.

3.3. Electrochemical performance of hydrazine on the PtNPs modified GCE

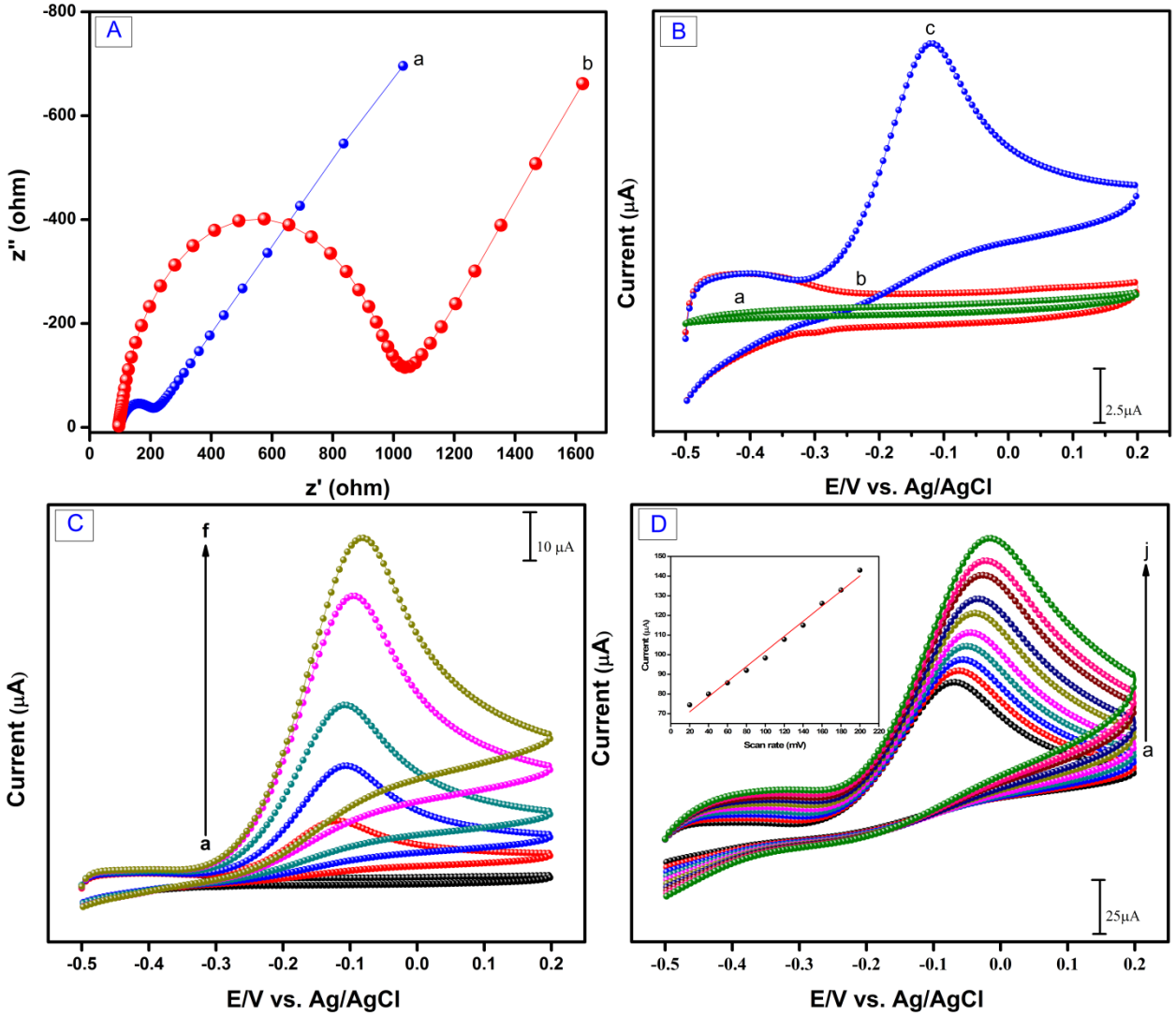

Figure 2 (A). the EIS spectrum of bare (a) Pt NPs/GCE (b) containing 0.1 M KCl solution with 5 mM $[Fe(CN)_6]^{3-/4-}$. (B) CVs response of various modified electrodes presence of bare (a) Pt NPs/GCE and absence of Pt NPs/GCE (c) of 200 µM hydrazine in 0.05M PBS pH-7 at scan rate 50 mVs^{-1}. (C) Different concentration of hydrazine from 0 to 500 µM (a-f). (D) Different scan rate from 20 to 200 mVs^{-1} (a-j) (inset: Ipa *vs.* scan rate).

Fig.2B shows the CVs response of the green synthesized Pt NPs modified GCE in the presence (bare GCE (a) and Pt NPs/GCE (c)) and absence of (Pt NPs (b)) 200µM hydrazine containing 0.05M phosphate buffer solution (PBS) pH-7 at a scan rate 50 mVs^{-1}. Fascinatingly, it is seen that the Pt NPs modified GCE does not show any oxidation peak in the selected potential window range of -0.5 to 0.2V, which is suggesting that the Pt NPs modified GCE was electrochemically inactive. Meanwhile, the presence of hydrazine a well-defined sharp oxidation peak (Fig.2B(c)) was observed in the onset potential of -0.3V at the same selected potential window range. On the reverse cycle, no reduction peak has been observed corresponding to the oxidation peak, which indicates that the electrochemical reaction is irreversible. The presence of hydrazine in without modified GCE was also studied there is

no oxidation peak was observed due to the unmodified GCE has no electrocatalytic activity towards hydrazine. The above all result suggests that the green synthesized PtNPs as excellent electron mediators and enhancing the electrochemical properties for the hydrazine oxidation. The electrochemical oxidation mechanism of hydrazine was discussed and detailed in formerly reported paper [18]. Fig.2C depicts the CVs of hydrazine solution in the various concentrations from 0-500 µM (a-f). The increasing the concentration of hydrazine the oxidation peak current was also increased, which is suggests that the Pt NPs has good electrocatalytic activity towards hydrazine.

3.4. Effect of scan rate

Fig.2D reveals the CVs of the Pt NPs/GCE with various scan rates containing 200 µM of hydrazine in PBS pH-7. It visibly shows that the anodic peak (Ipa) current was increased when increasing the scan rates from 20 to 200 mV (a-j) and the peak potential was shifted to positive side. The linear relationship plot was obtained with scan rate *vs.* Ipa (inset: Fig.2D) with linear regression equation as Ipa = 0.3841x + 63.276 (mV). The correlation coefficient of R^2= 990. The above result indicates that the overall electrochemical process is typical surface controlled process [19].

3.5. Calibration curve and interference studies

The amperometric performance of the Pt NPs to consecutive addition of hydrazine was further investigated under optimized from CVs experimental condition.

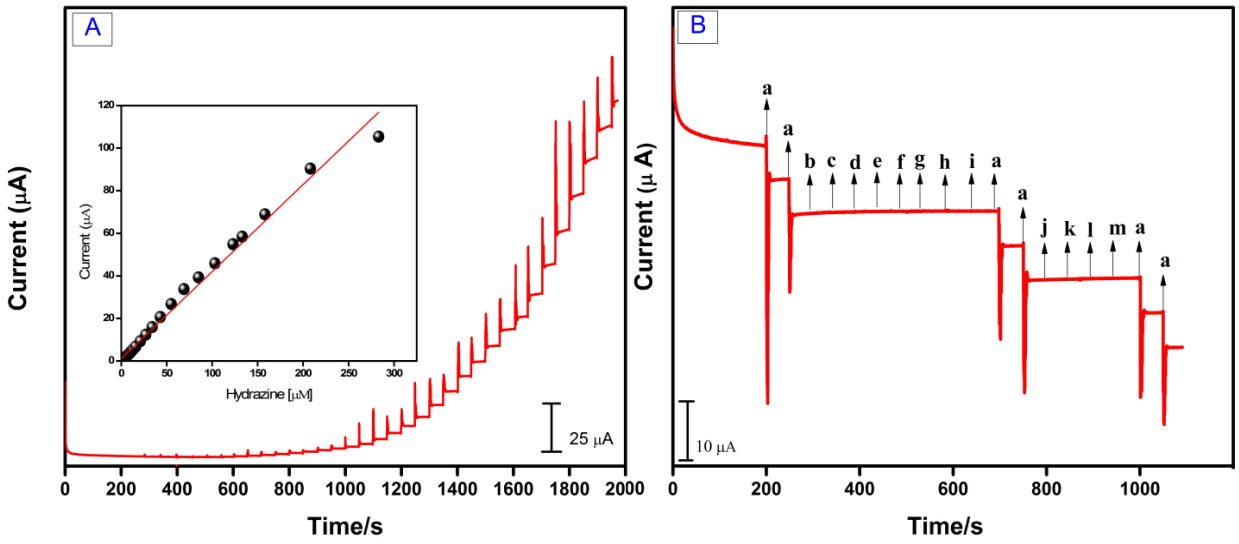

Figure 3.(A) Amperometric(i-t) response of PtNPs modified RDCE in PBS (pH-7) at applied potential -0.18 V of the successive addition of various concentration of hydrazine (0.01 to 953 µM) inset: linear relationship between Ipa *vs.* Hydrazine(µM) (B) Amperometric responses of Pt NPs/RDCE to successive additions of hydrazine (a),250 fold excess concentration of Ca^{2+} (b) Ba^{2+} (c) Cu^{2+} (d) Ni^{2+} (e) Cd^{2+} (f) Zn^{2+} (g) NO_2^- (h) NO_3^{2-} (i) and 50 fold excess of biological compounds DA (j) AA (k) UA (l) catachol (m).

An Amperometric technique is one of the better sensitive and higher resolution method compared than CVs technique. Based on the CVs optimized results, the amperometric (*i-t*) was recorded based on green synthesized Pt NPs modified RDCE with successive addition of various concentration of hydrazine to continuous stirred 0.05 M PBS (pH-7) at applied potential -0.18 V with rotation speed 1200 rpm. The strong amperometric response can be observed in each addition of hydrazine for the green synthesized Pt NPs modified RDCE and the oxidation peak current of hydrazine increased linearly and reached a steady state current. The amperometric responses attained a steady state signal with in 4s, suggests rapid electrocatalytic behavior. The anodic peak current was dependent on the hydrazine concentrations. The augmented sensing performances due to the excellent mass transport and the huge effective surface area resulting from the small size of the Pt NPs. The amperometric signal illustrated a linear correlation to hydrazine concentration in the range of 0.01-283μM (inset: Fig.3A), the linear regression equation was expressed as Ipa (μA) = 0.409 $C_{hydrazine}$ (μM) + 1.0812 with correlation coefficient (R^2 = 989). The detection limit and sensitivity of 7nm and 1.704 μA/μM/cm^2. The analytical performances such as limit of detection (LOD), applied potential, linear range and sensitivity of the proposed electrochemical sensor have been compared with previously reported hydrazine sensor and the comparative results are summarized in Table 1. From Table 1, it is obvious that the limit of detection, good sensitivity and lower onset applied potential of the green synthesized Pt NPs modified RDCE is comparable results for previously reported various modified electrodes for hydrazine determination.

The selectivity is very important for the electrochemical sensor. In order to investigate the selectivity based on green synthesized Pt NPs for hydrazine (a), 250 and 50 fold excess concentrations of Ca^{2+} (b) Ba^{2+} (c) Cu^{2+} (d) Ni^{2+} (e) Cd^{2+} (f) Zn^{2+} (g) NO_2^- (h) NO_3^{2-} (i) and biological compounds such as DA (j) AA (k) UA (l) catachol (m) were chosen for their possible interferences respectively (Fig.3B). The above results clearly confirmed that the aforementioned common metal ions and biological compounds have no interference to the determination of hydrazine. The proposed sensor exhibited has excellent selectivity towards hydrazine.

Table 1. Comparison of analytical performance of the proposed Green synthesized Pt NPs modified electrode with previously reported modified electrodes for hydrazine detection.

Modified Electrodes	Methods	Applied Potential (V)	Sensitivity (μA μM^{-1} cm^{-2})	Linear range (μM)	Limit of detection (μM)	Ref
AuPd NPs/GR	Amperometry	0.2	-	1-2185	0.2	20
Au/porous-TiO_2	Amperometry	0.2	0.17	2.5-500	0.5	21
ZnO/Au	Amperometry	0.3	1.6	66-415	0.06	22
Au/ZnO/WCNTs	Amperometry	0.2	0.042	0.5-1800	0.15	23
Au NPs-GPE	Amperometry	0.3	-	-	3.07	24
γ-$Fe_2O_3^o$/Au	Amperometry	0.18	0.06	0.02-11	0.006	25
Ni-DAP/Au-Pt NPs/NFs	Amperometry	0.35	-	0.2-85	0.1	26
(PANI/Pd)13 multilayers	CV	-0.22		0.2-350	0.05	27
Pd-Au NPs/GCE	Amperometry	-0.26	-	0.1-500	0.07	28

Pd/f-MWCNTs/GCE	Amperometry	0.27	-	10-70	1	29
Pt NPs/poly(taurine)/GCE	LSV	0.4	-	0.1–1000	5	30
Pt NPs/poly(BCP)/CNT/GCE	LSV	-0.28	-	0.5-1000	0.1	31
Mn_2O_3 nanorods	Amperometry	0.6	-	2-1300	1.1	32
Au NPs/TWEEN/GO	Amperometry	0.4	-	5-300	0.078	33
Pt NP BDD	Amperometry	-0.36		10-1000	3.3	34
Green synthesized Pt NPs/GCE	Amperometry	-0.18	1.704	0.01-283	0.007	This work

Au-Gold: Pd-palladium: GR-Graphene; TiO_2- Titanium dioxide; ZnO-Zinc oxide; WCNTs-Walled carbon nanotubes; Au NPs-Gold nanoparticles; GPE-Graphite pencil electrode; Fe_2O_3- Iron oxide; Ni-DAP-Nickel-2, 6-Diaminopyridine; Pt NPs-Platinum nanoparticles; NFs-Nanofibers; PANI-Polyaniline; GCE-Glassy carbon electrode; f-MWCNT-functionalized multiwalled carbon nanotube; BCP/CNT- Bromcresol purple/carbon nanotube; GO-Graphene oxide; Pt NP BDD-Platinum metal nanoparticles boron-doped diamond

3.6. Real sample analysis

The real time application of developed hydrazine sensor was studied towards the determination of hydrazine in various water samples. The various water samples was collected from various sources and known concentrations of hydrazine were spiked then directly used for the hydrazine determination. The standard addition method was followed to calculate the recoveries. The hydrazine spiked waters samples are successfully quantified by Pt NPs/GCE. The obtained recoveries were ranging from 98.7 % to 99.8 % for the hydrazine and results are summarized in Table. 2. The obtained results showed the satisfactory results.

Table 2. Determination of hydrazine in real samples using green synthesized Pt NPs/GCE

Sample	Added (µM)	Found[a] (µM)	Recovery (%)
Tap water	10	9.92	99.2
	20	19.89	99.4
Drinking water	10	9.94	99.4
	20	19.96	99.8
River water	10	9.87	98.7
	20	19.79	98.9

[a] Standard addition method

4. CONCLUSION

In conclusion, we have successfully developed green synthesized Pt NPs by using Qg leaves extract. The structure and morphology of Pt NPs were characterized by various spectroscopic and

analytical techniques such as UV-visible, TEM and FTIR. The crystalline structure of the as-prepared Pt NPs was confirmed by XRD technique. EIS technique was used to examine the interfacial properties of modified and unmodified electrodes. The green synthesized Pt NPs achieved an excellent electrocatalytic activity towards the electro-oxidation of hydrazine in terms of very low detection limit, wide linear range, lower onset oxidation potential and good sensitivity. The steady state current response measured by amperometric technique, the response for electrochemical oxidation of hydrazine was scrutinized within 4s. The practical applicability of the proposed chemical sensor was demonstrated in various water samples (Tap, river and drinking water). In future, the exclusive and excellent properties of our proposed chemical sensor can be widened into other significant applications.

References

1. R. Karthik, Shen-Ming Chen, A. Elangovan, P. Muthukrishnan, R. Shanmugam, Bih-Show Lou, *Journal of Colloid and Interface Science*, 468 (2016) 163-175.
2. A. Safavi, G. Absalan, F. Bamdad, *Analytica Chimica Acta*, 610 (2008) 243-248.
3. H. Kirchherr, *Journal of Chromatography B: Biomedical Sciences and Applications*, 617 (1993) 157-162.
4. M. George, K. Nagaraja, N. Balasubramanian, Analytical Letters, 40 (2007) 2597-2605.
5. M.C. Daniel, D. Astruc, *Chem. Rev*. 104 (2003) 293-346.
6. N. Karikalan, M. Velmurugan, S.M. Chen and K. Chelladurai**,** *ACS Appl. Mater. Interfaces*, DOI: 10.1021/acsami.6b07260
7. N. Karikalan, M. Velmurugan, S. M. Chen and K. Chelladurai, *RSC Adv,* 6 (2016) 48523.
8. R. Karthik, Yu-Shen Hou, Shen-Ming Chen, A. Elangovan, M. Ganesan, P. Muthukrishnan, *Journal of Industrial and Engineering Chemistry* 37 (2016) 330-339.
9. B. Zheng, T. Kong, X. Jing, T.O. Wubah, X. Li, D. Sun, F. Lu, Y. Zheng, J. Huang, Q. Li, *Journal of Colloid and Interface Science* 396 (2013) 138-145.
10. P. Velmurugan, J. Shim, K. Kim, B.T. Oh, *Materials letters* 174 (2016) 61-65.
11. A. Thirumurugan, P. Aswitha, C. Kiruthika, S. Nagarajan, A.N. Christy, *Materials Letters* 170 (2016) 175-178.
12. V.T.P. Vinod, P. Saravanan, B. Sreedhar, D. Keerthi Devi, R.B. Sashidhar, *Colloid Surface* B., 83 (2011) 291-298.
13. R. Venu, T.S. Ramulu, S. Anandakumar, V.S. Rani, C.G. Kim, *Colloid Surfaces* A 384 (2011) 733-738.
14. J.Y. Song, E.Y. Kwon, B.S. Kim, *Bioproc. Biosyst. eng*., 33 (2010) 159-164.
15. R.S. Bai, T.E. *Water Res*. 36 (2002) 1224-1236.
16. X. Huang, H. Wu, X. Liao, B. Shi, *Green Chem*. 12 (2009) 395-399.
17. B. Evgenij and M.J. Ross. Impedance spectroscopy theory, experiment, and applications. New Jersy: Wiley; 2005
18. P. K. Kannan Stanislav, A. Moshkalev, and C. Sekhar Rou, *RSC Adv*., 6 (2016) 11329.
19. R. Madhu, B. Dinesh, S.M. Chen, R. Saraswathi and V. Mani**,** *RSC Adv*, 5 (2015) 54379.
20. Y. Liu, B. Li, W. Wei, Q. Wan and N. Yang, *Adv. Mater. Res*, 704 (2013) 246.
21. G. Wang, C. Zhang, X. He, Z. Li, X. Zhang, L. Wang and B. Fang, *Electrochim. Acta,* 55 (2010) 7204.
22. W. Sultana, S. Ghosh and B. Eraiah, *Electroanalysis,* 24 (2012) 1869.

23. C. Zhang, G. Wang, Y. Ji, M. Liu, Y. Feng, Z. Zhang and B. Fang, *Sens. Actuators B,* 150 (2010) 247.
24. Md. AbdulAziz and A.N. Kawde, *Talanta*, 115 (2013) 214.
25. Y. You, Y. Yang and Z. Yang, *J. Solid State Electrochem*, 17 (2013) 701.
26. A. Azadbakht and A.R. Abbasi, *Nano Micro Lett*, 2 (2010) 296.
27. H. Lin, J. Yang, J. Liu, Y. Huang, J. Xiao, and X. Zhang, *Electrochimica Acta*, 90 (2013) 382.
28. M. Shamsipur, Z. Karimi, M. A. Tabrizi, and A. Shamsipur, *Electroanalysis*, 26 (9) (2014) 2001.
29. M. Rajkumar, C. P. Hong, and S.M. Chen, *Int. J. Electrochem. Sci*, 8(4) (2013) 5262.
30. Ç. C. Koçak, A. Altın, B. Aslışen and S. Koçak, *Int. J. Electrochem. Sci*, 11 (2016) 233.
31. S. Koçak, A. Altın and Ç. C. Koçak, *Analytical Letters*, 49(7) (2016) 1015.
32. B. Zhou, J.Yang and X. Jiang, *Mater. Lett*, 159 (2015) 362.
33. W. Lu, R. Ning, X. Qin, Y.i. Zhang, G. Chang, S. Liu, Y. Luo and X. Sun, J. *Hazard. Mater,* 197 (2011) 320.
34. R.B. Channon, J.C. Newland, A.W.T. Bristow, A.D. RAY, J.V. Macpherson, *Electroanalysis*, 25 (2013) 2613.